https://doi.org/10.17221/96/2025-SWR

Linking seasonal fractional vegetation cover dynamics with soil organic carbon stock and microbial indicators in tropical agroecosystems

Ni Made Trigunasih[1], Moh Saifulloh[2], Ida Bagus Putu Bhayunagiri[1], Zulkarnain Zulkarnain[3]*

[1]*Department of Soil Sciences, Faculty of Agriculture, Udayana University, Denpasar, Indonesia*
[2]*Spatial Data Infrastructure Development Centre (PPIDS), Udayana University, Denpasar, Indonesia*
[3]*Agroecotechnology Study Program, Faculty of Agriculture, Mulawarman University, Samarinda, East Kalimantan, Indonesia*

**Corresponding author: m.saifulloh@unud.ac.id*

Citation: Trigunasih N.M., Saifulloh M., Bhayunagiri I.B.P., Zulkarnain Z. (2026): Linking seasonal fractional vegetation cover dynamics with soil organic carbon stock and microbial indicators in tropical agroecosystems. Soil & Water Res., 21: 107–120.

Abstract: Reliable indicators of early soil biological change remain limited in tropical agroecosystems, where soil organic carbon (SOC) stocks may respond more slowly than microbial processes. We evaluated whether seasonal vegetation dynamics derived from Sentinel-2 fractional vegetation cover (FVC) are associated with spatial variation in SOC stock and microbial indicators in Jembrana, Bali, Indonesia. We mapped seasonal FVC from 2019 to 2024 and derived site-level metrics of mean cover and temporal variability (standard deviation, anomaly, coefficient of variation, and a temporal stability index). In July 2023, we sampled topsoil (0–30 cm) at 12 sites representing contrasting land uses and topographic settings. We calculated SOC stock from organic carbon concentration, bulk density, and sampling depth, and measured basal respiration and culturable microbial density (colony-forming units, CFU). Vegetation cover peaked consistently during the wet season (December to February), and mean site FVC ranged from 0.31 to 0.99. Mean FVC showed positive but non-significant associations with culturable microbial density (Spearman's $\rho = 0.48$, $P = 0.114$) and basal respiration ($\rho = 0.29$, $P = 0.361$), whereas higher vegetation variability metrics tended to coincide with lower culturable microbial density ($\rho = -0.43$ to -0.51, $P = 0.090$ to 0.163). SOC stock showed near-zero coefficients and no statistical evidence of association with vegetation metrics ($\rho = 0.09$, $P = 0.781$) or microbial indicators ($\rho = 0.01$, $P = 0.975$). Principal component analysis of FVC traits explained 99.65% of the variance and separated sites along a gradient from stable, high cover to more variable, lower cover. Overall, FVC stability metrics captured spatial differences that were directionally consistent with microbial indicators, but associations were not statistically significant in this dataset ($n = 12$). Larger, replicated studies with repeated soil sampling are required to evaluate whether seasonal FVC metrics have robust predictive utility for SOC stock and soil biological indicators.

Keywords: biomass; carbon dynamics; land degradation; microbial activity; PCA; soil respiration; tropical soils

Supported by the Research and Community Service Institute (LPPM) of Universitas Udayana for providing funding through the 2024 Senior Academic Research Grant under the Universitas Udayana PNBP Budget Implementation Document (DIPA), as stated in the Research Implementation Assignment Agreement Letter No. B/255.614/UN14.4.A/PT.01.03/2024, dated April 17, 2024. Additional thanks are given for the continued support in the 2025 fiscal year through the Universitas Udayana PNBP DIPA, as stated in the Research Implementation Assignment Agreement Letter No. B/229.51/UN14.4.A/PT.01.03/2025, dated April 28, 2025.

https://doi.org/10.17221/96/2025-SWR

Rising greenhouse gases, global climate change, and environmental degradation threaten ecosystem stability (Bhatti et al. 2024; Saifulloh et al. 2025a). Increasing and protecting vegetation biomass can mitigate climate change by sequestering atmospheric carbon, producing oxygen, regulating water flow, and reducing erosion in hazard-prone landscapes (Trigunasih et al. 2026). Biomass integrates above- and belowground organic matter and indicates ecosystem productivity and carbon cycling (Zhang et al. 2023). Accurate, time-resolved biomass quantification is therefore essential for evaluating environmental change and guiding sustainable land management.

Since the Industrial Revolution, anthropogenic emissions have increased atmospheric CO_2 by about 31%. Cumulatively, fossil-fuel combustion contributed ~270 ± 30 Pg C and land-use change contributed ~136 ± 55 Pg C. Soil organic carbon (SOC) losses alone added an estimated 78 ± 12 Pg C, largely from degraded soils that lost 30–40 Mg C/ha (Lal 2004). Despite these losses, global vegetation biomass has recovered slowly, increasing by 0.50 ± 0.20 Pg C/year in recent decades, reflecting a decoupling between terrestrial growth and atmospheric carbon fluxes (Yang et al. 2023).

Beyond mitigation, SOC underpins soil structure, fertility, and biological function. Recent synthesis work estimates ~899 Pg C in the upper 1 m of non-permafrost mineral soils, only 42% of the mineralogical storage potential (Georgiou et al. 2022). A meta-analysis of more than 13 000 field experiments shows that optimising SOC increases yields of rice, maize, and wheat, although gains remain smaller than those from nitrogen fertilisation (Wang et al. 2024).

Microbial biomass and necromass constitute a large share of SOC, often more than half, highlighting the central role of microbial activity and respiration in processing plant-derived inputs during the growing season (Jia et al. 2022). However, many studies explain SOC distribution using static factors such as land use, elevation, and climate, with limited attention to temporal vegetation dynamics. For example, Tibetan grasslands often exceed 40 g/kg SOC relative to adjacent forests or croplands (Ma et al. 2022). In Ethiopia, SOC ranges from 7.24 Mg C/ha in lowland grasslands to 2.34 Mg C/ha in degraded areas (Seifu et al. 2021). In Nepal, elevation explains 58% of SOC variability (Malla et al. 2022). In Indonesian mangroves, natural stands store nearly twice the SOC of reclaimed ponds, underscoring strong land-use effects (Agustriani et al. 2024).

These spatial insights often overlook seasonal changes in vegetation biomass, particularly in the tropics where two to three distinct growing seasons occur each year. During the wet season, rapid growth increases litterfall, root turnover, and rhizodeposition, which elevate microbial respiration and can enhance SOC accrual. Seasonal dynamics are fundamental to soil carbon processes but remain underrepresented in integrated studies of vegetation and soils. Remote sensing supports consistent monitoring of fractional vegetation cover (FVC) (Anees et al. 2022; Han et al. 2023). Combining Sentinel-2 imagery with cloud platforms such as Google Earth Engine enables rapid, large-scale analysis of seasonal vegetation change (Sunarta & Saifulloh 2022; Susila et al. 2024; Saifulloh et al. 2025b; Sunarta et al. 2025).

FVC provides a practical proxy for biomass, and seasonal FVC can illuminate links between vegetation dynamics and soil carbon processes. Nevertheless, no study has systematically linked seasonal FVC with SOC, microbial respiration, and microbial abundance in tropical agroecosystems. Our research aimed to analyse spatiotemporal FVC patterns from 2019 to 2024 and evaluate their relationships with SOC stock, basal respiration, and culturable microbial density (CFU/g dry soil) in tropical agroecosystems. Given the limited sample size, our objective is exploratory: to test whether FVC mean and stability metrics are directionally consistent with soil biological indicators and to assess their potential for stratifying sites for targeted monitoring and hypothesis generation.

MATERIAL AND METHODS

Area of study

We conducted this study in Jembrana Regency, Bali Province, Indonesia, a region with diverse landforms and lithologies (Figure 1A). The landscape includes alluvial plains, fluviomarine plains, beach ridges, foot slopes, and volcanic middle and lower slopes. Elevation ranges from 3.59 to 340.59 m above sea level, and slope ranges from 1.69% to 49.74%. These gradients influence erosion rates, organic matter accumulation, soil water movement, and microbial activity (Trigunasih & Saifulloh 2023; Soniari et al. 2024).

Geologically, the area comprises three major lithological units: (*i*) quaternary volcanic products (lava, breccia, tuff) from recent volcanism on mountain slopes and undulating terrains; (*ii*) the Jembrana volcanic formation from older volcanic processes

https://doi.org/10.17221/96/2025-SWR

on steep middle and lower volcanic slopes; and (*iii*) alluvial deposits of sand, gravel, silt, and clay from fluvial sedimentation in low-lying coastal and river-valley settings (Sinarta et al. 2016; Diara et al. 2022).

This geological complexity and geomorphic diversity drive variability in soil fertility by altering parent material composition, solum depth, and the soil's capacity to retain organic matter (Lira-Martins et al. 2022). Table 1 lists the dominant land uses (e.g., rice fields, mixed gardens, dryland forests) alongside their associated geomorphological and lithological settings. We designed the soil sampling to span this full range of landforms, lithologies, and land uses, enabling a robust assessment of spatiotemporal variation in SOC stock, basal respiration, and culturable microbial density in tropical agricultural land.

Soil sampling and laboratory analysis

Soil sampling was conducted in July 2023 across 12 representative sites selected to capture variations in land use, elevation, slope, and canopy cover, as shown in Table 1. A purposive sampling approach was employed to ensure that each location reflected distinct biophysical conditions of the landscape. At each site, a 50 m radius was delineated, within which five subsamples were collected and composited into a single representative bulk sample (~1 kg fresh soil).

Soil samples were collected from the 0–30 cm topsoil horizon using a hand auger with a 15-cm diameter barrel. This sampling depth was specifically selected to capture the zone of maximal microbial activity and biomass accumulation, a stratification pattern consistent with established tropical soil protocols (Li et al. 2023; Pei et al. 2025). Furthermore, this depth interval aligns with previous agricultural studies which identify the top 30 cm as the primary reservoir of soil nutrients and organic matter availability in cultivated lands (Kartini et al. 2023, 2024; Trigunasih & Saifulloh 2022; Trigunasih et al. 2023). This method ensured the retrieval of sufficient soil volume while minimising site disturbance. To ac-

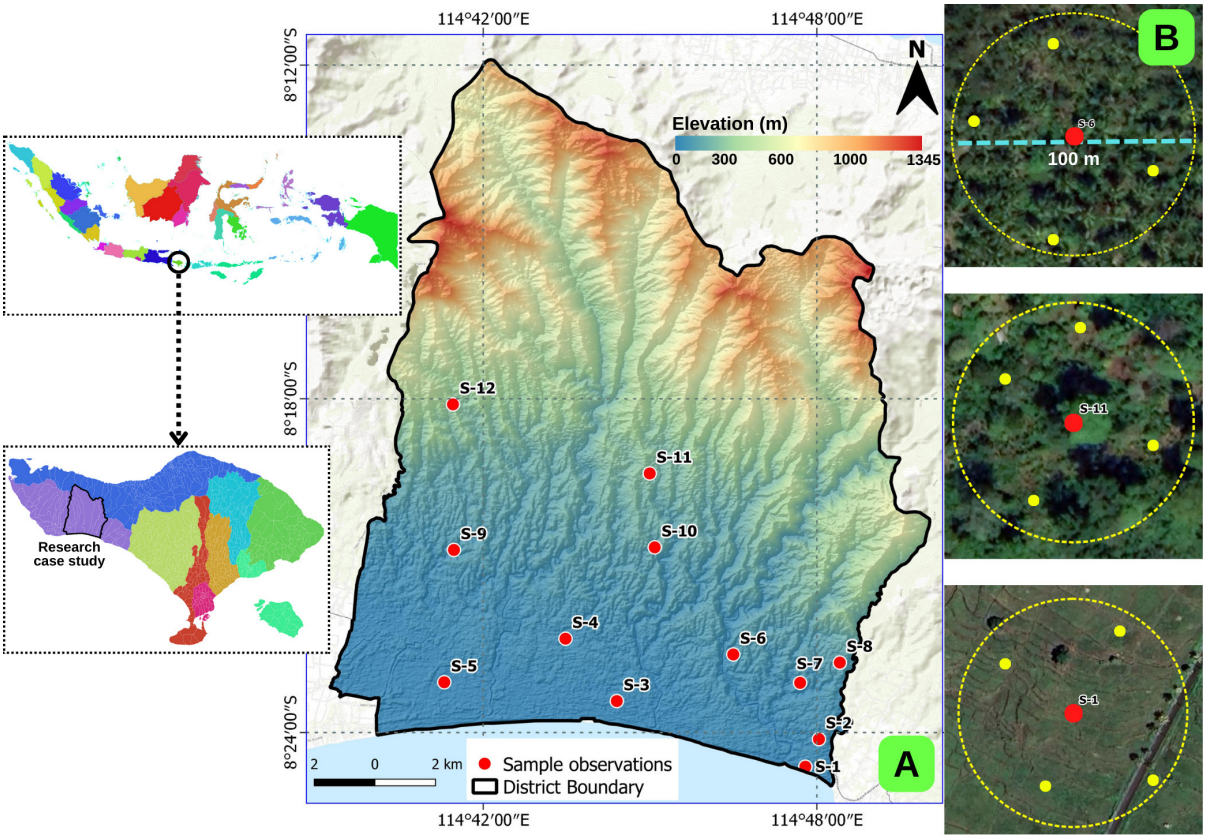

Figure 1. Research location in Jembrana District, Bali, Indonesia (A) showing sample observation points (B) satellite imagery of selected sample plots (S-6, S-11, S-1) with 50-meter observation buffers (yellow circles) and subsample points (yellow dots)

https://doi.org/10.17221/96/2025-SWR

Table 1. Site characteristics by land use, geology, and topography

Sample	Land use	Geological unit	Landform	Soil sub-order	Soil order	Average elevation (m)	Average slope (%)
S-1	paddy fields	quaternary volcanic products	alluvial plain	fluvents	Entisols	12.95	1.69
S-2	paddy fields	quaternary volcanic products	undulating plain	udepts	Inceptisols	35.32	5.86
S-3	paddy fields	quaternary volcanic products	beach ridge	psamments	Entisols	9.68	7.83
S-4	paddy fields	quaternary volcanic products	footslope	udepts	Inceptisols	27.23	10.01
S-5	paddy fields	alluvial deposits	fluvio-marine plain	fluvents	Entisols	3.59	3.44
S-6	perennial plants	quaternary volcanic products	fluvio-marine plain	udepts	Inceptisols	40.85	14.65
S-7	perennial plants	Jembrana volcanic formation	undulating plain	udepts	Inceptisols	65.11	22.38
S-8	perennial plants	Jembrana volcanic formation	footslope	udepts	Inceptisols	113.96	24.38
S-9	perennial plants	quaternary volcanic products	lower volcanic slope	udepts	Inceptisols	65.89	29.06
S-10	perennial plants	quaternary volcanic products	upper volcanic slope	udepts	Inceptisols	151.2	37.47
S-11	secondary dryland forest	Jembrana volcanic formation	lower volcanic slope	udepts	Inceptisols	250.48	40.78
S-12	primary dryland forest	Jembrana volcanic formation	middle volcanic slope	udepts	Inceptisols	340.59	49.74

count for spatial heterogeneity in organic inputs, vegetation cover and root density were characterised at each sampling point.

After field collection, we homogenised each composite soil sample and split it into two subsamples.

Microbial analyses. We placed ~300 g fresh soil immediately into a sterile, airtight vacuum container, maintained it at < 4 °C, and transported it to the laboratory within 24 hours. These conditions follow standard microbial-preservation protocols that recommend storage at 2–4 °C to maintain viability and minimise respiration (ISO 10381-6:2009; USDA NRCS Soil Quality Test Kit Guide).

Chemical analyses. We air-dried the remaining ~700 g soil for 4–7 days depending on ambient humidity, gently disaggregated it, and passed it through a 2 mm sieve to remove coarse fragments, following routine laboratory practice (ISO 11464:2006).

C-organic (%). We determined C-organic by the Walkley and Black wet oxidation method using potassium dichromate ($K_2Cr_2O_7$) and concentrated sulfuric acid (H_2SO_4), followed by back-titration with ferrous ammonium sulphate. This procedure estimates oxidizable carbon and is widely applied to tropical topsoils (Walkley & Black 1934).

Bulk density (BD). Bulk density was measured independently from the composite auger sample using undisturbed cores to preserve soil structure. At each site, we collected six intact cores using stainless steel rings (5 cm diameter and 5 cm height) to represent the 0–30 cm layer. Cores were taken as separate increments at 0–5, 5–10, 10–15, 15–20, 20–25, and 25–30 cm within the site buffer. Each core was oven-dried at 105 °C for 24 h, and BD was calculated as oven-dry mass divided by core volume (g/cm^3). Site-level BD was calculated as the mean of the six cores and used for SOC stock estimation.

Basal respiration and culturable microbial density. Soil basal respiration was quantified to estimate total metabolic activity. We incubated fresh soil samples in hermetically sealed vessels containing 0.1 M NaOH traps to capture evolved CO_2, which was subsequently titrated with HCl following the alkali absorption method (Anderson 1982).

https://doi.org/10.17221/96/2025-SWR

To assess the viable, metabolically active fraction of the microbial community, we determined culturable microbial density (CFU/g dry soil) using the serial dilution and spread plate technique on nutrient agar. Plates were incubated at 28 ± 2 °C for 48 h (Zuberer 1994). While we acknowledge that culture-dependent methods capture a specific subset of the total soil microbiome (the great plate count anomaly), this metric was specifically selected to monitor the zymogenous (fast-growing) heterotrophic community that responds rapidly to labile carbon inputs derived from seasonal vegetation dynamics (Pepper et al. 2011).

Data calculation

Soil organic carbon (SOC). Soil organic carbon stock is a key indicator of soil quality and ecosystem function. We calculated SOC stock by combining laboratory-determined organic carbon concentration with bulk density and sampling depth. SOC stock was expressed in megagrams per hectare (Mg/ha) to support spatial comparison and integration with satellite-derived vegetation metrics. The SOC was calculated using the following Equation (1):

$$SOC_{stock} = OC \times BD \times depth \quad (1)$$

where:
OC – organic carbon (%);
BD – bulk density (g/cm^3);
depth – vertical depth of soil collected in cm.

Seasonal fractional vegetation cover (FVC). We used Sentinel-2 Level-2A surface reflectance from COPERNICUS/S2_SR_HARMONIZED in Google Earth Engine (GEE: https://earthengine.google.com/) to map vegetation cover at 10 m using Band 4 (Red, 664.5 nm) and Band 8 (NIR, 835.1 nm) (Gorelick et al. 2017). Field observation points were uploaded as a FeatureCollection and buffered by 50 m to represent local vegetation. We masked clouds and shadows with the Sentinel-2 scene classification layer (SCL), excluding pixels labelled cloud, shadow, snow, or noise and retaining vegetated, bare soil, or water pixels. We computed the normalised difference vegetation index (NDVI) following Rouse et al. (1973) (Equation 2) and derived FVC using the normalised NDVI transformation (Equation 3), where NDVI_min (≈ 0.15) and NDVI_max (≈ 0.90) were used in this study as reference values representing bare or sparsely vegetated surfaces and dense vegetation, respectively.

For each 50-m buffer, we extracted seasonal (DJF/MAM/JJA/SON) mean FVC for 2019–2024 (n = 24 seasonal observations per site) and calculated summary metrics of central tendency and temporal variability: FVC_Mean (mean of the seasonal series), FVC_Std (standard deviation), FVC_CoV (FVC_Std divided by FVC_Mean), and FVC_Anomaly (mean absolute deviation of seasonal FVC from the site's multi-year seasonal mean). We also computed the temporal stability index (TSI) from the same seasonal series, expressed such that higher TSI values indicate lower temporal stability (greater variability) and lower values indicate more stable vegetation cover.

$$NDVI = \frac{B8 - B4}{B8 + B4} \quad (2)$$

$$FVC = \left(\frac{NDVI - NDVI_{min}}{NDVI_{max} - NDVI_{min}} \right)^2 \quad (3)$$

where:
$NDVI_{min}$, $NDVI_{max}$ – the NDVI thresholds for bare soil (~0.15) and dense vegetation (~0.90), respectively;
$B8$ – Band 8: near infrared (NIR), central wavelength 842 nm in the Sentinel-2 product;
$B4$ – Band 4: red, central wavelength 665 nm in the Sentinel-2 product.

Statistical analysis and visualisation. We examined relationships between vegetation metrics and soil variables (SOC stock, basal respiration, and culturable microbial density). Monotonic relationships were tested using Spearman's rank correlation and are reported as Spearman's ρ with two-sided P-values; statistical significance was evaluated at α = 0.05 (MacFarland & Yates 2016). To summarise gradients among vegetation metrics, we performed principal component analysis (PCA) on z-score standardised FVC traits. To evaluate similarity among sites across vegetation and soil indicators, we applied Ward's hierarchical clustering to the combined set of z-score standardised variables (FVC traits plus SOC stock, basal respiration, and culturable microbial density). All analyses were conducted in Python (version 3.13) using reproducible scripts executed in JupyterLab (Mendez et al. 2019)

$$\rho_s = 1 - \frac{6\sum d_i^2}{n(n^2 \mid 1)} \quad (4)$$

where:
d_i –the rank difference for each paired observation;

https://doi.org/10.17221/96/2025-SWR

n – the number of observations; positive values indicate direct association and negative values indicate inverse association.

$$C = \frac{1}{n-1} Z^{\top} Z \quad (5)$$

where:

C – the covariance matrix of Z;

Z – the z-score standardised data matrix (columns centred and scaled);

n – the number of observations.

RESULTS

Seasonal fractional vegetation cover. Seasonal FVC followed a consistent annual cycle from 2019 to 2024 (Figure 2), with higher values in December-January-February (DJF) and lower values in June-August (JJA), consistent with the regional wet-dry seasonality. Deviations from this pattern, including the DJF 2023 decline, indicate interannual variability in canopy cover without attributing a specific driver.

The heatmap of site-level FVC across seasons and years (Figure 3) shows that S-2, S-3, and S-5 maintained persistently low cover (< 0.5), indicating sparse vegetation and muted seasonality. S-5 exhibited a distinct space-time anomaly in SON 2023 (FVC = 0.15), indicating a transient reduction in vegetation cover relative to other seasons and sites.

Violin plots of FVC metrics (Figure 4) summarise mean cover (FVC_Mean), variability (FVC_Std), seasonal anomaly (FVC_Anomaly), the coefficient of variation (FVC_CoV), and temporal stability (TSI). FVC_Mean ranged from 0.31 to 0.99, confirming pronounced spatial heterogeneity. S-3 and S-5 combined low means (0.31 and 0.36) with high variability indicators (CoV > 0.45, Anomaly > 0.6), indicating comparatively higher temporal variability in vegetation cover across seasons. In contrast, S-6 and S-11 had high FVC_Mean (> 0.95) with low CoV and low Anomaly, indicating stable, seasonally responsive vegetation.

TSI values corroborated these patterns. S-3 and S-5 had TSI > 1.5, indicating strong temporal instability and stress-prone vegetation. Sites with TSI < 0.5 maintained stable cover across seasons. Across all sites, low FVC_Mean tended to coincide with higher variability metrics (CoV and TSI), indicating that these descriptors capture a gradient from stable, high-cover sites to more variable, lower-cover sites.

Linking vegetation metrics with soil organic carbon and microbial indicators. Figure 5 summarises Spearman correlations between FVC metrics and soil variables. Mean FVC showed positive correlations with culturable microbial density ($\rho = 0.48$, $P = 0.114$) and basal respiration ($\rho = 0.29$, $P = 0.361$), but neither relationship was statistically significant at $\alpha = 0.05$. Vegetation instability metrics were negatively correlated with culturable microbial density, includ-

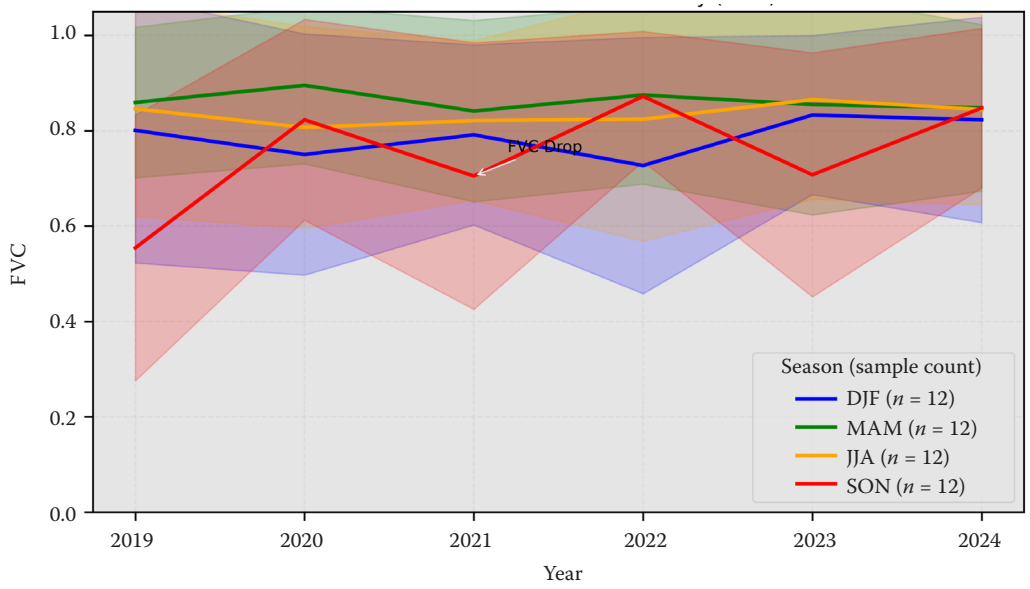

Figure 2. Seasonal trends of fractional vegetation cover (FVC) from 2019 to 2024 with standard deviation shading
DJF – December–February; MAM – March–May; JJA – June–August; SON – September–November

https://doi.org/10.17221/96/2025-SWR

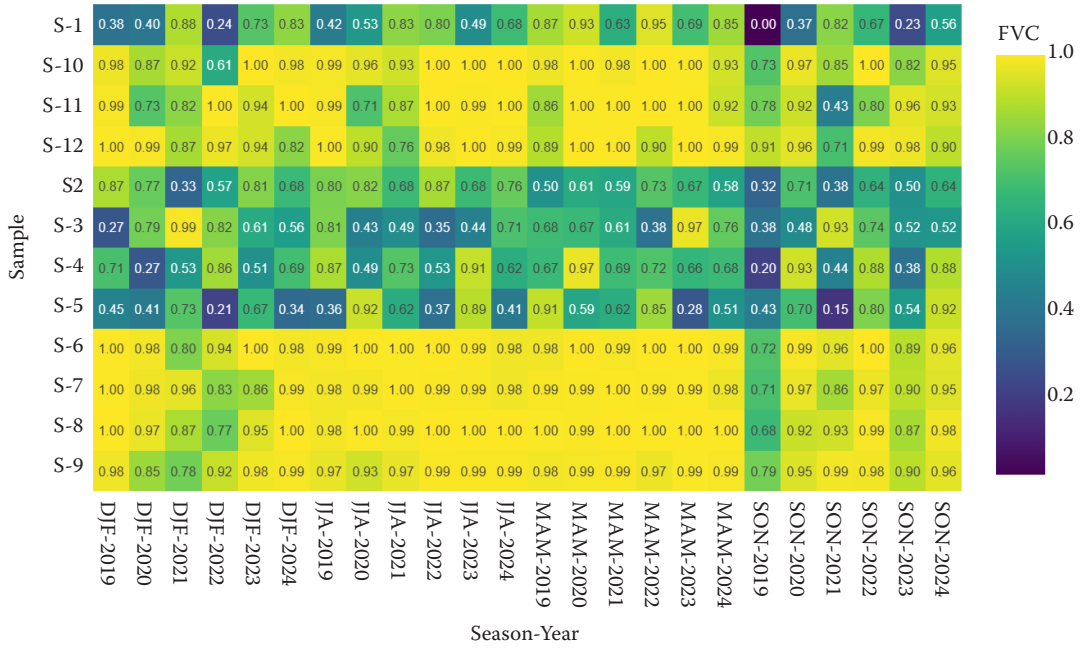

Figure 3. Heatmap of fractional vegetation cover (FVC) values per sample across seasonal-year combinations
S – sample site; DJF – December–February; MAM – March–May; JJA – June–August; SON – September–November

ing coefficient of variation (ρ = −0.48, P = 0.114), anomaly (ρ = −0.51, P = 0.090), and temporal stability index (ρ = −0.43, P = 0.163). SOC stock showed near-zero coefficients and no statistical evidence of association with mean FVC (ρ = 0.09, P = 0.781) or culturable microbial density (ρ = 0.01, P = 0.975). Basal respiration was moderately correlated with SOC (ρ = 0.37, P = 0.236) and with culturable microbial density (ρ = 0.51, P = 0.090). Overall, the correlation directions were consistent with higher microbial indicators under denser and more stable vegetation, but these relationships were not statistically significant in this dataset (n = 12).

PCA and vegetation soil clustering. We applied PCA to reduce the FVC metrics and to identify dominant gradients in vegetation dynamics (Fernandez et al. 2017). The first two components explained 99.65% of total variance: PC1 accounted for 92.36% and PC2 for 7.29% (Figure 6), capturing the principal patterns in vegetation structure.

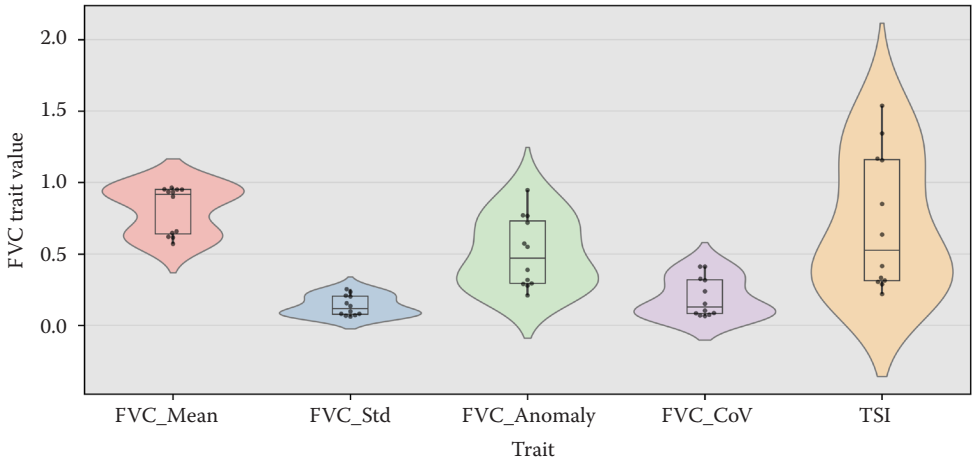

Figure 4. Violin plot of fractional vegetation cover (FVC) statistical traits showing distribution density and interquartile ranges
Std – standard deviation; CoV – coefficient of variation; TSI – temporal stability index

https://doi.org/10.17221/96/2025-SWR

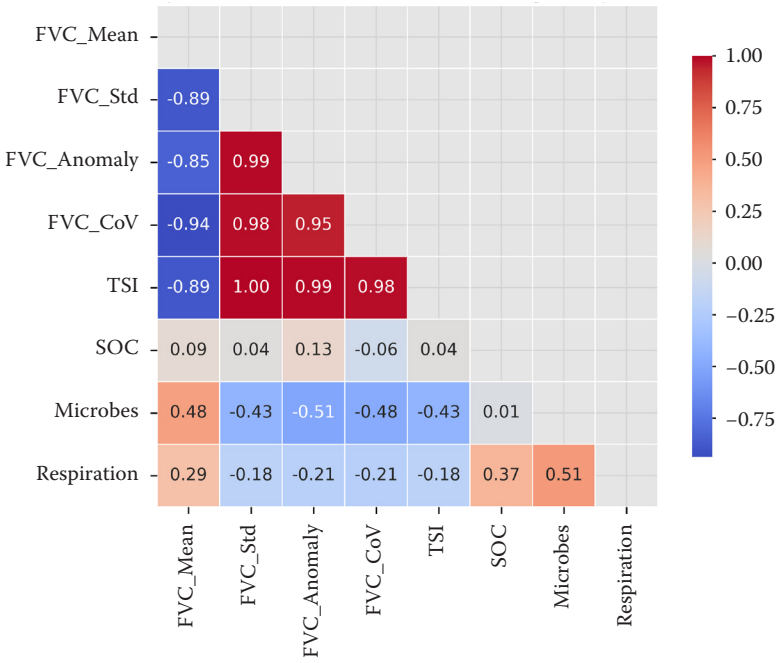

Figure 5. Spearman correlation matrix between fractional vegetation cover (FVC) traits and soil biological properties
Std – standard deviation; CoV – coefficient of variation; TSI – temporal stability index; SOC – soil organic carbon

Loadings distinguished two axes of variation. PC1 loaded strongly on FVC_Anomaly, FVC_Std, FVC_CoV, and the TSI, representing vegetation instability. PC2 loaded mainly on FVC_Mean, representing stable vegetation productivity. This biplot delineated a gradient from productive, stable canopies to stressed, unstable vegetation.

Projecting site scores into PCA space revealed three groups. Group 1 (blue; S-6, S-9, S-11) combined high FVC_Mean with low CoV, Anomaly,

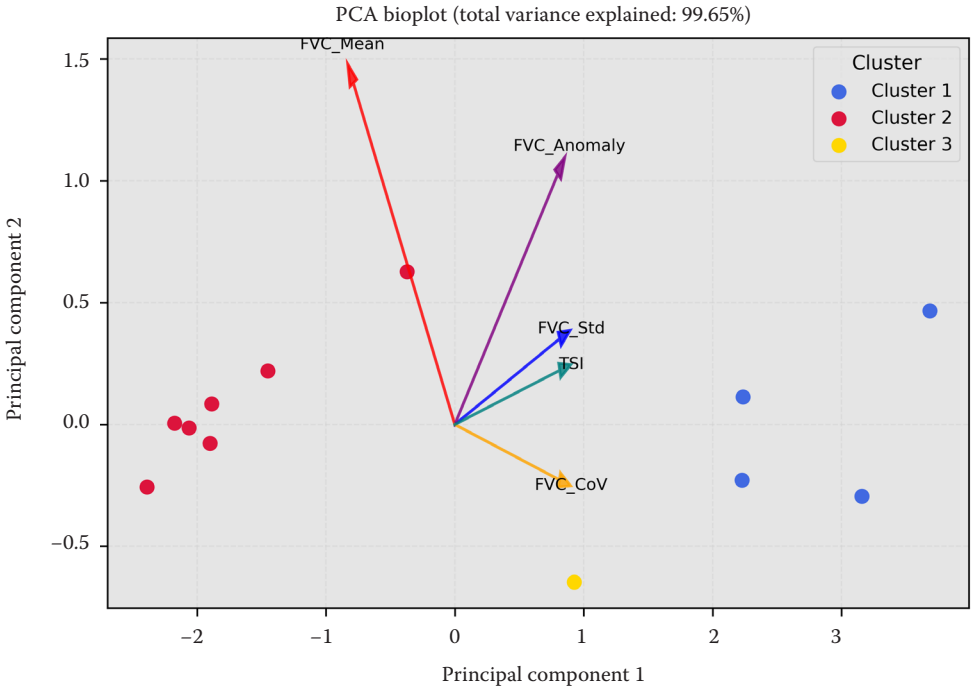

Figure 6. Principal component analysis (PCA) biplot of fractional vegetation cover (FVC) traits showing three vegetation clusters
Std – standard deviation; CoV – coefficient of variation; TSI – temporal stability index

https://doi.org/10.17221/96/2025-SWR

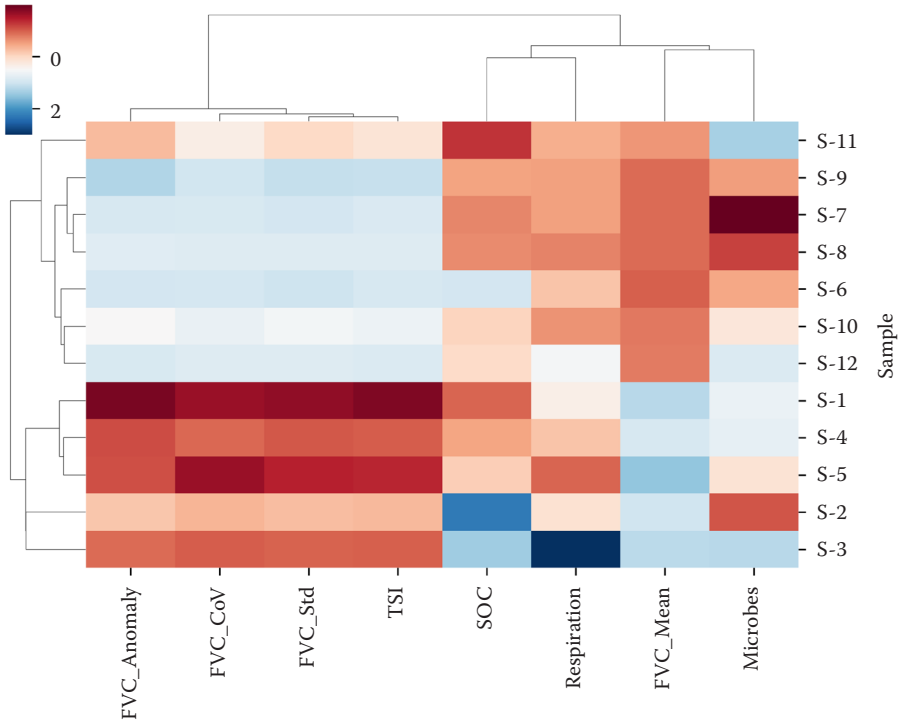

Figure 7. Clustergram of z-score normalised fractional vegetation cover (FVC) traits and soil biological indicators
Std – standard deviation; CoV – coefficient of variation; TSI – temporal stability index; SOC – soil organic carbon

and TSI, indicating stable, minimally disturbed landscapes with strong seasonal responsiveness. Group 2 (S-1, S-3, S-5) showed lower mean cover and higher temporal variability, consistent with more disturbed or intensively managed vegetation states that warrant independent field confirmation. Group 3 (Yellow) occupied intermediate positions with moderate values for all metrics, consistent with transitional ecosystems under moderate stress or early recovery.

Hierarchical clustering on z-score-standardised variables corroborated the PCA groupings (Figure 7). Cluster 2 exhibited low z-scores for SOC and respiration, supporting biological and vegetative degradation. Cluster 1 showed high FVC and elevated microbial respiration, consistent with a stable, biologically active system. Cluster 3 remained intermediate across variables.

This clustering framework supports management zoning. Cluster 1 aligns with conservation and maintenance priorities, cluster 2 identifies critical restoration targets, and cluster 3 suits adaptive interventions. Integrating vegetation indicators with soil biological traits provides an efficient basis for monitoring ecosystem condition, prioritizing restoration, and guiding long-term land-use planning. Future work should extend the time series with additional remote sensing data, broaden microbial profiling, and model degradation risk under varying climate and land-use scenarios.

DISCUSSION

Seasonal FVC followed the expected wet-season increase and dry-season decline, and sites with higher mean cover tended to show higher soil biological indicators (basal respiration and culturable microbial density), although these relationships were not statistically significant in this dataset. Specifically, FVC_Mean showed a positive but non-significant association with basal respiration (Spearman's $\rho = 0.29$, $P = 0.361$), consistent with the general mechanism that greater plant-derived carbon inputs (litter and rhizodeposition) can support higher microbial activity (Berhongaray et al. 2019). Evidence from vegetation restoration studies further suggests that increasing plant carbon inputs can promote SOC accumulation through microbial pathways, with microbial biomass carbon and microbial necromass carbon identified

https://doi.org/10.17221/96/2025-SWR

as key predictors of SOC gains (Wang et al. 2025). In line with process-centric soil health frameworks, management-driven variation in biomass inputs has also been reported to explain a substantial share of observed changes in soil condition (Rubio et al. 2025). Taken together, these lines of evidence support interpreting seasonal FVC dynamics as a useful, remotely sensed proxy for potential carbon-input gradients, while recognising that the present pilot dataset does not establish causality or mechanistic pathways.

In contrast, sites with lower and more variable cover (e.g., S-3 and S-5) tended to show lower culturable microbial density and lower basal respiration (Ren et al. 2018). The sensitivity of biological properties to such vegetation changes appears to exceed that of chemical properties. In a comprehensive meta-analysis of 144 studies, Mgelwa et al. (2025) revealed that deforestation and land cover change induced a profound decline in microbial biomass and enzyme activities, whereas chemical properties like pH remained relatively stable. Mechanistically, Zhou et al. (2023) explain this response by showing that during the first 22 years of post-agricultural restoration, microbial biomass accumulates significantly faster than total SOC because rapid microbial growth is induced by labile litter components. Together, these studies suggest that soil biological indicators can respond more rapidly than bulk SOC to shifts in organic inputs, but the present pilot dataset is not sufficient to infer early-warning performance.

PCA separated a stability axis (FVC_Mean) from an instability gradient (CoV, Anomaly, TSI), and hierarchical clustering mapped these gradients onto functional groups, from stable and biologically active to degraded and unstable. This multivariate structure mirrors findings that temperature, topography, and canopy attributes drive ecosystem classification (Massaccesi et al. 2020). The recovery of these degraded zones requires understanding the microbial driving forces. Chen et al. (2024) found that afforestation in subtropical zones effectively increases SOC storage because plant nutrients stimulate microbial enzymatic activities, transitioning soil from nitrogen limitation to phosphorus limitation. Similarly, Zhou et al. (2025) observed that vegetation restoration in degraded lands increased microbial necromass carbon by over 40% highlighting that the recovery of the microbial community is the precursor to long-term soil health.

Clusters with stable FVC and high respiration signal conservation priorities, whereas degraded clusters require urgent restoration, supporting the view that SOC alone is too inert for real-time soil health assessment and should be paired with responsive biological metrics (Wiesmeier et al. 2019). The ecological significance of this stability is supported by Yang et al. (2025) who showed in alpine grasslands that management practices enhancing vegetation cover also improved the spatial stability of organic carbon pools. They found that reduced disturbance increased the weights of vegetation characteristics on soil stability. Additionally, Yang et al. (2025) established that vegetation succession enhances organic matter not only through litter inputs but by reshaping bacterial communities toward taxa that stabilise carbon via physicochemical interactions. Thus, the stable clusters identified in our PCA likely represent zones where bacterial communities have successfully established a stable regulatory pathway for carbon sequestration.

Stable FVC aligned with higher respiration, and organic matter additions can shift SOC chemistry, reduce recalcitrance, and enhance enzyme activity, strengthening vegetation-soil feedbacks (Luan et al. 2020). However the pathway from active vegetation to stable soil carbon is complex and time-dependent. Zhao et al. (2025) utilised biomarker approaches to show that while vegetation succession increases microbial-derived carbon, it can take 90 to 100 years for this necromass to achieve a stable contribution to soil sequestration. This reinforces our argument that short-term FVC metrics are proxies for the active process of sequestration rather than the stored result. Although some climax forests show SOC gains even when vegetation restoration lowers carbon use efficiency due to controls such as pH and phosphorus availability (Shi et al. 2024), our non-forest tropical setting was more strongly governed by seasonal vegetation dynamics.

In this dataset, SOC stock showed near-zero coefficients and no statistical evidence of association with FVC (Spearman's $\rho = 0.09$, $P = 0.781$) or with culturable microbial density ($\rho = 0.01$, $P = 0.975$), consistent with SOC integrating longer-term inputs than captured by a single sampling campaign. This statistical decoupling confirms that SOC functions as a long-term integrator of carbon inputs, responding too slowly to capture the rapid environmental shifts reflected in vegetation dynamics. This limitation of static SOC monitoring is a global challenge described by Padarian et al. (2022), who argue that because SOC is a dynamic property driven by land

https://doi.org/10.17221/96/2025-SWR

cover changes, static baselines fail to capture rapid losses. They noted that tropical regions account for almost 50% of global SOC loss due to land cover change, necessitating the type of time-series remote sensing approach we employed. Furthermore, Kumar and Sharma (2025) found significant seasonal variability in carbon stocks in semi-arid wetlands, with depletion occurring during pre-monsoon seasons. This suggests that static measurements miss critical seasonal fluxes that FVC monitoring can capture. Additionally, Liu et al. (2022) noted that environmental variables like precipitation often have strong interactive effects on SOC that mask simple linear relationships, further complicating the use of SOC as a standalone short-term indicator. Furthermore, sampling depth constraints inherent to standard inventories can obscure SOC sensitivity, a limitation recently highlighted by Dubeux et al. (2024).

Consequently, dynamic vegetation stability metrics may complement static SOC measurements by providing time-resolved information on canopy cover that can be evaluated alongside soil biological indicators. This approach is vital for addressing conservation gaps as Núñez-Hidalgo et al. (2025) emphasise the need to identify and protect threatened ecosystems that store significant carbon but fall outside current protected networks. Pairing remote-sensing indicators (e.g., FVC) with soil biological measurements (e.g., basal respiration and culturable microbial density) may help stratify heterogeneous landscapes for targeted field assessment, but it does not by itself establish near-real-time detection of degradation. We acknowledge certain limitations in this remote-sensing approach: FVC relies on canopy reflectance and may not fully capture subsurface dynamics, including litter quality, root turnover, and microbial necromass accumulation. Additionally, the structural heterogeneity typical of evergreen or perennial agroforestry systems may introduce noise into stability metrics, potentially confounding cluster delineation. Future research should therefore integrate direct biomass measurements, carbon flux monitoring, and seasonal litterfall analysis to validate these remote signals. Nonetheless, this pilot analysis illustrates how seasonal FVC metrics can be used to structure sampling and generate testable hypotheses about soil biological patterns in tropical agricultural landscapes.

Nonetheless, this pilot analysis illustrates how seasonal FVC metrics can be used to structure sampling and generate testable hypotheses about soil biological patterns in tropical agricultural landscapes

CONCLUSION

Seasonal FVC in Jembrana showed a consistent wet-season peak from 2019 to 2024, and FVC-derived stability metrics separated sites along a gradient from stable, high-cover to more variable, lower cover. Correlations between vegetation metrics and microbial indicators were directionally consistent with higher microbial activity under denser and more stable vegetation, but these relationships were not statistically significant in this dataset (n = 12). SOC stock showed near-zero coefficients and no statistical evidence of association with vegetation metrics or microbial indicators at this sample size and time scale. Overall, seasonal FVC metrics can support landscape stratification and hypothesis generation, but predictive applications require larger, replicated studies with repeated sampling.

Acknowledgements. We thank the entire team who assisted with field data collection, and we are especially grateful to the anonymous reviewers for their valuable suggestions and constructive feedback on this manuscript.

REFERENCES

Agustriani F., Iskandar I., Yazid M., Ulqodry T.Z.I., Fauziyah F. (2024): Soil organic carbon across varying habitat conditions in the mangrove ecosystem in Sembilang National Park, South Sumatra, Indonesia. Biodiversitas Journal of Biological Diversity, 25: 4603–4612.

Anderson J.P.E. (1982): Soil respiration. Methods of Soil Analysis: Part 2 Chemical and Microbiological Properties, 9: 831–871.

Anees S.A., Zhang X., Shakeel M., Al-Kahtani M.A., Khan K.A., Akram M., Ghramh H.A. (2022): Estimation of fractional vegetation cover dynamics based on satellite remote sensing in Pakistan: A comprehensive study on the FVC and its drivers. Journal of King Saud University – Science, 34: 101848.

Berhongaray G., Cotrufo F.M., Janssens I.A., Ceulemans R. (2019): Below-ground carbon inputs contribute more than above-ground inputs to soil carbon accrual in a bioenergy poplar plantation. Plant and Soil, 434: 363–378.

Bhatti U.A., Bhatti M.A., Tang H., Syam M.S., Awwad E.M., Sharaf M., Ghadi Y.Y. (2024): Global production patterns: Understanding the relationship between greenhouse gas emissions, agriculture greening and climate variability. Environmental Research, 245: 118049.

Chen Y., Dai Z., Yang S., Wang F., Yue H., Peng S., Cao W. (2024): Effects of different restored vegetation on soil

https://doi.org/10.17221/96/2025-SWR

organic carbon pools in subtropic erosive lands: Insights from stable carbon isotopes. Forest Ecology and Management, 564: 122040.

Diara I.W., Suyarto R., Saifulloh M. (2022): Spatial distribution of landslide susceptibility in new road construction Mengwitani-Singaraja, Bali-Indonesia: Based on geospatial data. International Journal of GEOMATE, 23: 95–103.

Dubeux Jr, J.C.B., Lira Junior M.deA., Simili F.F., Bretas I.L., Trumpp K.R., Bizzuti B.E., Garcia L., Oduor K.T., Queiroz L.M.D., Acuña J.P. (2024): Deep soil organic carbon: A review. Cabi Reviews, 19: 1.

Fernandez N.F., Gundersen G.W., Rahman A., Grimes M.L., Rikova K., Hornbeck P., Ma'ayan A. (2017): Clustergrammer, a web-based heatmap visualization and analysis tool for high-dimensional biological data. Scientific Data, 4: 1–12.

Georgiou K., Jackson R.B., Vindušková O., Abramoff R.Z., Ahlström A., Feng W., Harden J.W., Pellegrini A.F.A., Polley H.W., Soong J.L., Riley W.J., Torn M.S. (2022): Global stocks and capacity of mineral-associated soil organic carbon. Nature Communications, 13: 3797.

Gorelick N., Hancher M., Dixon M., Ilyushchenko S., Thau D., Moore R. (2017): Google Earth Engine: Planetary-scale geospatial analysis for everyone. Remote Sensing of Environment, 202: 18–27.

Han H., Yin Y., Zhao Y., Qin F. (2023): Spatiotemporal variations in fractional vegetation cover and their responses to climatic changes on the Qinghai-Tibet Plateau. Remote Sensing, 15: 2662.

Jia S., Liu X., Lin W., Li X., Yang L., Sun S., Hui D., Guo J., Zou X., Yang Y. (2022): Tree roots exert greater influence on soil microbial necromass carbon than above-ground litter in subtropical natural and plantation forests. Soil Biology and Biochemistry, 173: 108811.

Kartini N.L., Saifulloh M., Trigunasih N.M., Narka I.W. (2023): Assessment of soil degradation based on soil properties and spatial analysis in dryland farming. Journal of Ecological Engineering, 24: 368–375.

Kartini N.L., Saifulloh M., Trigunasih N.M., Sukmawati N.M.S., Mega I. (2024): Impact of long-term continuous cropping on soil nutrient depletion. Ecological Engineering & Environmental Technology (EEET), 25: 18–29.

Kumar S., Sharma L.K. (2025): Assessing spatial and seasonal variability in soil organic carbon fractions of teal carbon in semi-arid Ramsar wetlands of India as a natural climate solution. Discover Soil, 2: 66.

Lal R. (2004): Soil carbon sequestration to mitigate climate change. Geoderma, 123: 1–22.

Li L., Hosseiniaghdam E., Drijber R., Jeske E., Awada T., Hiller J., Kaiser M. (2023): Conversion of native grassland to coniferous forests decreased stocks of soil organic carbon and microbial biomass. Plant and Soil, 491: 591–604.

Lira-Martins D., Nascimento D.L., Abrahão A., de Britto Costa P., D'Angioli A.M., Valézio E., Rowland L., Oliveira R.S. (2022): Soil properties and geomorphic processes influence vegetation composition, structure, and function in the Cerrado Domain. Plant and Soil, 476: 549–588.

Liu H., Sun Z., Dong Y., Yang H., He P., Yu B., Ye H., Li S., Zhou L. (2022): Precipitation drives the accumulation of soil organic carbon in the sandy desert of the Junggar Basin, Northwest China. Ecological Indicators, 142: 109224.

Luan H., Gao W., Huang S., Tang J., Li M., Zhang H., Chen X., Masiliūnas D. (2020): Organic amendment increases soil respiration in a greenhouse vegetable production system through decreasing soil organic carbon recalcitrance and increasing carbon-degrading microbial activity. Journal of Soils and Sediments, 20: 2877–2892.

Ma Z., Qin W., Wang Z., Han C., Liu X., Huang X. (2022): A meta-analysis of soil organic carbon response to livestock grazing in grassland of the Tibetan Plateau. Sustainability (Switzerland), 14: 14065.

MacFarland T.W., Yates J.M. (2016): Spearman's rank-difference coefficient of correlation. In: Introduction to Nonparametric Statistics for the Biological Sciences Using R. Springer: 249–297.

Malla R., Neupane P.R., Köhl M. (2022): Modelling soil organic carbon as a function of topography and stand variables. Forests, 13: 2–14

Massaccesi L., De Feudis M., Leccese A., Agnelli A. (2020): Altitude and vegetation affect soil organic carbon, basal respiration and microbial biomass in Apennine forest soils. Forests, 11: 710.

Mendez K.M., Pritchard L., Reinke S.N., Broadhurst D.I. (2019): Toward collaborative open data science in metabolomics using Jupyter Notebooks and cloud computing. Metabolomics, 15: 125.

Mgelwa A.S., Ngaba M.J.Y., Hu B., Gurmesa G.A., Mwakaje A.G., Nyemeck M.P.B., Zhu F., Qiu Q., Song L., Wang Y. (2025): Meta-analysis of 21st century studies shows that deforestation induces profound changes in soil characteristics, particularly soil organic carbon accumulation. Forest Ecosystems, 12: 100257.

Núñez-Hidalgo I., Pfeiffer M., Lira E., Alaniz A.J., Gaxiola A. (2025): Assessing the impact of landcover change on soil organic carbon stocks in Chile: Implications for terrestrial ecosystems and conservation policies. Journal of Applied Ecology, 62: 2636–2656.

Padarian J., Stockmann U., Minasny B., McBratney A.B. (2022): Monitoring changes in global soil organic carbon stocks from space. Remote Sensing of Environment, 281: 113260.

https://doi.org/10.17221/96/2025-SWR

Pei J., Li J., Luo Y., Rillig M.C., Smith P., Gao W., Li B., Fang C., Nie M. (2025): Patterns and drivers of soil microbial carbon use efficiency across soil depths in forest ecosystems. Nature Communications, 16: 5218.

Pepper I., Gerba C.P., Gentry T., Maier R.M. (2011): Environmental Microbiology. London, Academic Press.

Ren C., Wang T., Xu Y., Deng J., Zhao F., Yang G., Han X., Feng Y., Ren G: (2018): Differential soil microbial community responses to the linkage of soil organic carbon fractions with respiration across land-use changes. Forest Ecology and Management, 409: 170–178.

Rubio V., Nunez A., Berger A., van Es H. (2025): Biomass inputs drive agronomic management impacts on soil health. Agriculture, Ecosystems & Environment, 378: 109316.

Rouse J.W., Haas R.H., Schell J.A., Deering D.W. (1973): Monitoring the vernal advancement and retrogradation (green wave effect) of natural vegetation. Progress Report RSC 1978-1. College Station, Texas A&M University/ NASA.

Saifulloh M., Santosa I.G.N., Sunarta I.N., Ambarawati I.G.A.A., Sudarma I.M., As-Syakur A.R. (2025a): Mapping GHG emission vulnerability using convolutional autoencoder and multi-sensor satellite In Bali, Indonesia. Geography, Environment, Sustainability, 18: 135–144.

Saifulloh M., Sunarta I.N., Baiquni M., Trigunasih N.M., Adikampana I. (2025b): Linking annual land subsidence to built-up density across coastal tourism zones via Sentinel-1 differential interferometric synthetic aperture radar. Ecological Engineering & Environmental Technology (EEET), 26: 326–336.

Seifu W., Elias E., Gebresamuel G., Khanal S. (2021): Impact of land use type and altitudinal gradient on topsoil organic carbon and nitrogen stocks in the semi-arid watershed of northern Ethiopia. Heliyon, 7: e06770.

Shi J., Deng L., Wu J., Bai E., Chen J., Shangguan Z., Kuzyakov Y. (2024): Soil organic carbon increases with decreasing microbial carbon use efficiency during vegetation restoration. Global Change Biology, 30: e17616.

Sinarta I., Rifa'i A., Fathani T.F., Wilopo W. (2016): Geotechnical properties and geology age on characteristics of landslides hazards of volcanic soils in Bali, Indonesia. International Journal of GEOMATE, 11: 2595–2599.

Soniari N.N., Trigunasih N.M., Sumarniasih M.S., Saifulloh M. (2024): Exploring soil erodibility: Integrating field surveys, laboratory analysis, and geospatial techniques in sloping agricultural terrains. Journal of Degraded and Mining Lands Management, 12: 6533–6544.

Sunarta I.N., Saifulloh M. (2022): Coastal tourism: Impact for built-up area growth and correlation to vegetation and water indices derived from Sentinel-2 remote sensing imagery. Geo Journal of Tourism and Geosites, 41: 509–516.

Sunarta N., Arida I., Trigunasih N.M., Michele K., Saifulloh M. (2025): Overtourism triggered built-up expansion over a decade in Canggu, Bali. Ecological Engineering & Environmental Technology, 26: 1–14.

Susila K.D., Trigunasih N.M., Saifulloh M. (2024): Monitoring agricultural drought in savanna ecosystems using the vegetation health index – Implications of climate change. Ecological Engineering & Environmental Technology (EEET), 25: 54–67.

Trigunasih N.M., Saifulloh M. (2022): Correlation between soil nitrogen content and NDVI derived from Sentinel-2A satellite imagery. Jurnal Lahan Suboptimal: Journal of Suboptimal Lands, 11: 112–119.

Trigunasih N.M., Saifulloh M. (2023): Investigation of soil erosion in agro-tourism area: Guideline for environmental conservation planning. Geographia Technica, 18: 19–28.

Trigunasih N.M., Narka I.W., Saifulloh M. (2023): Measurement of soil chemical properties for mapping soil fertility status. International Journal of Design and Nature and Ecodynamics, 18: 1381–1390.

Trigunasih N.M., Saifulloh M., Sunarta I.N. (2026): Geospatial identification of soil erosion hotspots exacerbating the catastrophic flash flood in Bali , Indonesia. Geographia Technica, 21: 105–126.

Walkley A., Black I.A. (1934): An examination of the degtjareff method for determining soil organic matter, and a proposed modification of the chromic acid titration method. Soil Science, 37: 29–37.

Wang S., Sun N., Zhang S., Longdoz B., Wellens J., Meersmans J., Colinet G., Wu L., Xu M. (2024): Soil organic carbon storage impacts on crop yields in rice-based cropping systems under different long-term fertilisation. European Journal of Agronomy, 161: 127357.

Wang Y., Li D., Yang Q., Lu J., Jiang Y., Su T., Milinga A., Shi Q., Liu W., Yang H. (2025): Effects of plant carbon inputs and soil microbe on soil organic carbon accumulation in different tropical vegetation restoration strategies. Ecological Engineering, 215: 107616.

Wiesmeier M., Urbanski L., Hobley E., Lang B., von Lützow M., Marin-Spiotta E., van Wesemael B., Rabot E., Ließ M., Garcia-Franco N., Wollschläger U., Vogel H.J., Kögel-Knabner I. (2019): Soil organic carbon storage as a key function of soils – A review of drivers and indicators at various scales. Geoderma, 333: 149–162.

Yang H., Ciais P., Frappart F., Li X., Brandt M., Fensholt R., Fan L., Saatchi S., Besnard S., Deng Z., Bowring S., Wigneron J.P. (2023): Global increase in biomass carbon stock dominated by growth of northern young forests over past decade. Nature Geoscience, 16: 886–892.

Yang H., Sun Z., Lu Q., Gao W., Bai Y. (2025): Analysis of the effects of seasonal rest grazing on the stability

https://doi.org/10.17221/96/2025-SWR

of soil organic carbon pools and its driving factors in alpine grasslands of Northern Xizang. Journal of Soils and Sediments, 25: 2896–2915.

Zhang X., Zhou Y., Ji Y., Yu M., Li X., Duan J., Wang Y., Gao J., Guo X. (2023): Climate factors affect above-belowground biomass allocation in broad-leaved and coniferous forests by regulating soil nutrients. Plants, 12: 3926.

Zhao Z., Qin Y., Wu Y., Chen W., Wang H., Chen J., Yang J., Liu G., Xue S. (2025): Microbial necromass carbon drives soil organic carbon accumulation during long-term vegetation succession. Journal of Applied Ecology, 62: 932–944.

Zhou H., Qu Q., Xu H., Wang M., Xue S. (2025): Effects of vegetation restoration on soil microbial necromass carbon and organic carbon in grazed and degraded sandy land. Journal of Environmental Management, 382: 125380.

Zhou J., Sun T., Shi L., Kurganova I., de Gerenyu V.L., Kalinina O., Giani L., Kuzyakov Y. (2023): Organic carbon accumulation and microbial activities in arable soils after abandonment: A chronosequence study. Geoderma, 435: 116496.

Zuberer D.A. (1994): Recovery and enumeration of viable bacteria. Methods of Soil Analysis: Part 2 Microbiological and Biochemical Properties, 5: 119–144.

Received: July 29, 2025
Accepted: February 12, 2026
Published online: March 31, 2026